inter•noise 96
25th Anniversary Congress – Liverpool

INCE: 31.1

NOISE BARRIERS WITH REACTIVE SURFACES

K Fujiwara (1) & D C Hothersall (2)

(1) Department of Acoustic Design, Kyushu Institute of Design, 9-1 Shiobaru, 4-chome, Fukuoka-shi, Japan, (2) Department of Civil and Environmental Engineering, University of Bradford, Bradford, BD7 1DP, UK

1. INTRODUCTION

Barriers are now widely used for the alleviation of noise nuisance, particularly from road traffic. In some situations, for example when visual intrusion is an important factor, it is desirable to find alternative methods of improving efficiency of a noise barrier without increasing the height. Improved designs of this nature have been proposed e.g. [1,2] which generally involve a modification to the upper edge of the barrier.

The performance of noise barriers can ultimately only be verified in field trials, but site and atmospheric conditions make controlled comparison of the performance of different designs difficult and expensive. Some form of modelling provides a controlled environment. Numerical modelling is efficient and the use of boundary element methods allows details of cross sectional shape and surface cover of barriers to be considered. The computing resources required for these calculations generally means that they are restricted to two dimensions. In this paper the boundary element modelling method will be used to study the effects of applying pressure release type surfaces to T-shaped barrier designs.

2. MODELLING METHOD

The numerical modelling method used has been described elsewhere [3]. It involves the reformulation of the Helmholtz equation as an integral equation in which the integral, taken over the surface of the barrier, is solved by a boundary element approach. The model is two-dimensional and assumes a point source of sound which, in three-dimensions, is equivalent to an infinite coherent line source lying parallel to the infinite barrier of uniform cross section and surface covering along the length.

The ground is an infinite plane and the ground and barrier surfaces are assumed rigid. The insertion loss is calculated at single frequencies, defined by $IL = 20\log_{10}(P_g/P_b)$, where P_g is the acoustic pressure at the receiver point with the ground present and P_b is the pressure at the same point after the introduction of the barrier.

3. RESULTS AND DISCUSSION

Source and receiver positions were taken in the ground surface, at 8.0 and 50 m from the centre line of the barrier respectively. Source and receiver positions in the ground were used so that the spectra produced are characteristic of the diffracting edge of the barrier and are not complicated by the effects of interference between direct sound and that reflected from the ground. For all cases the total height of the barrier was 3.0 m and the cap width was 1.0 m. The thickness of the cap and the supporting wall was 0.1 m. In Fig. 1 spectra of insertion loss at the receiver point are shown, calculated at 1/9th-octave centre frequencies. Curves are given for conditions when the plane upper surface of the

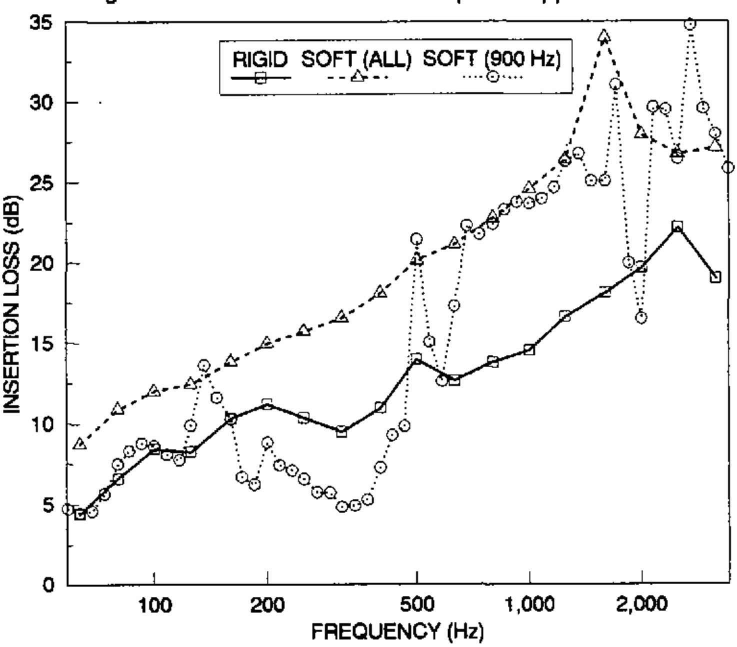

Fig. 1. Insertion loss spectra for a T-shaped barrier with an upper surface which is a)rigid, b)soft for *all frequencies*, and c)as shown in Fig.2.

The computations were performed at frequency 1000 Hz. The results are represented by the transfer function, defined as the sound pressure level relative to free field.

For the analytic computation, we used four sound rays, with a spherical wave diffraction coefficient derived by Hadden and Pierce [8], and a spherical wave reflection coefficient [9] for the ground reflections (see [3,10]). For the PE computation we used both the Crank-Nicholson PE (CNPE) and the Green's function PE (GFPE). The agreement between CNPE, GFPE and diffraction theory is excellent.

Various other comparisons between PE and a diffraction model were reported in Ref. [10]. These comparisons include systems with wide barriers, double screens, and rectangular barriers with an absorbing top surface. In most cases, good agreement was obtained.

Figure 4 shows the effect of atmospheric refraction. The PE results in this figure were computed for the same system as before. For the atmosphere we used a logarithmic sound speed profile $c(z) = c_0 + b \ln(z/z_0+1)$, with ground-level sound speed $c_0 = 343$ m/s, a roughness length $z_0 = 0.1$ m typical for grassland, and a parameter $b = 0$, 1 and 2 m/s. The results show that with increasing wind speed, the sound pressure level behind the screen first decreases and then increases.

Figure 5 shows PE results for the 1000 Hz octave band, up to a range of 5 kilometers [11]. The computations were performed for a system with a logarithmic sound speed profile with $b = 1.1$ m/s. We used two ground types: a ground with an impedance typical for grassland (see

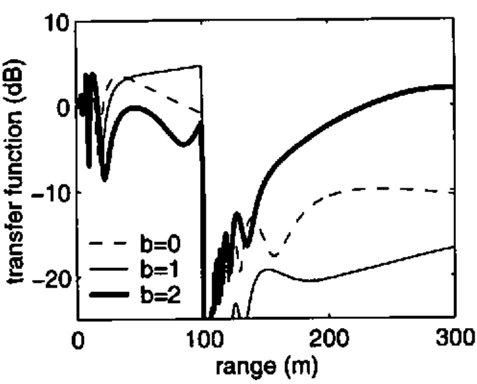

Fig. 4. Transfer function versus horizontal range, at 1000 Hz (single frequency), for atmosphere with $b = 0$, 1 and 2 m/s.

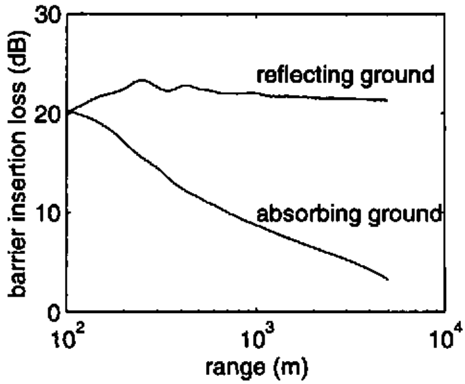

Fig. 5. Barrier insertion loss versus horizontal range, for 1000 Hz octave band, for a downward refracting atmosphere.

Ref. 11), and a reflecting ground. We used a height of 1.5 meters for the source and the receiver. A thin vertical screen with a height of 5 meters was located at 30 meters from the source. The figure shows the barrier insertion loss as a function of range. For the absorbing ground, the insertion loss decreases with increasing range. For the reflecting ground, the insertion loss remains approximately constant with increasing range. This difference in barrier efficiency between absorbing and reflecting ground can be explained qualitatively in terms of curved sound rays [11].

References

[1] K.E.Gilbert and M.J.White, J. Acoust. Soc. Am. 85, 630 (1989)
[2] M.West, K.Gilbert and R.A.Sack, Appl. Acoustics 37, 31 (1992)
[3] E.M.Salomons, J. Acoust. Soc. Am. 95, 3109 (1994)
[4] A.D.Pierce, Acoustics (American Institute of Physics, New York, 1981)
[5] K.E.Gilbert and M.J.White, Proc. Third Int. Symposium on Long Range Sound Propagation, March 28-30 (Jackson, Mississippi, 1988)
[6] K.Gilbert and X.Di, J. Acoust. Soc. Am., 94, 2343 (1993)
[7] M.E.Delany and E.N.Bazley, Appl. Acoustics 3, 105 (1970)
[8] J.W.Hadden and A.D.Pierce, J. Acoust. Soc. Am. 69, 1266 (1981)
[9] K.Attenborough et al, J. Acoust. Soc. Am. 68, 1493 (1980)
[10] E.M.Salomons, submitted to Acta Acustica
[11] E.M.Salomons, accepted for publication in Appl. Acoustics

barrier is a) rigid (Neumann boundary condition), with a surface impedance of unity, and b) of the 'soft' or pressure release type (Dirichelet boundary condition) with a surface impedance of -1 for all frequencies. Insertion loss increases with frequency as expected and the difference between the insertion loss for the soft and the rigid surfaces is of the order of 5.0 dB at lower frequencies and 10.0 dB at higher frequencies. A practical method of producing a soft surface over a limited range of frequencies has been considered by Fujiwara [4]. This is to construct wells in the surface, of depth $(\lambda / 4 + c)$, where λ is the wavelength of the sound and c is the end correction. Fig. 2 shows a construction of this type which was incorporated in the cap of the noise barrier. The depth of the wells is 0.095 m which is expected to produce a phase change of π in the reflected waves of normally incident waves with a frequency of 900 Hz.

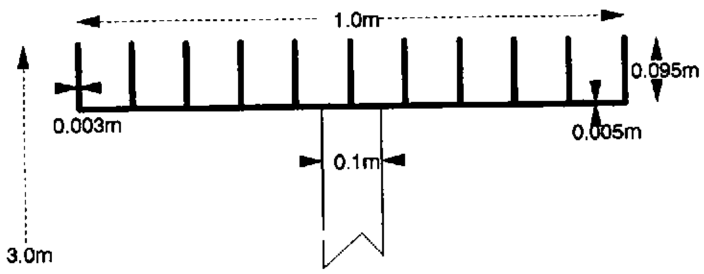

Fig. 2. Upper surface of a T-shaped barrier containing wells which are tuned to give pressure cancellation at the mouth at a frequency of 900 Hz.

The spectrum of the insertion loss for this barrier is also shown in Fig. 1. In the region from approximately 600 Hz to 1500 Hz the spectrum achieves the same value of insertion loss as for a soft surface. The dip in the spectrum around 2000 Hz may be associated with a pressure maximum which is expected at the mouth of the wells at twice the design frequency. The reasons for the oscillation in the spectrum at about 500 Hz are not clear. At lower frequencies, between 160 and 500 Hz, the barrier is less efficient than for a rigid cap. The dip in the spectrum is probably associated with the generation of a surface wave. This wave decays at a rate of $d^{-1/2}$ and exists for the propagation of spherical waves above boundaries for which the surface admittance has a finite and negative ($e^{-i\omega t}$ time dependence) imaginary part.

Simulations of the effect of the barrier were carried out assuming that the upper surface was plane, with a surface admittance given by

$$\beta_s = \frac{1}{(r_s + i\cot(k\ell))} \tag{1}$$

where k is the wave number and ℓ is the effective depth of the wells. The admittance has a negative imaginary part for frequencies below the design frequency of the wells. In Fig. 3 insertion loss spectra obtained using this expression, with $\ell = 0.95$ m and with $r_s = 0.0$ and 0.1 are shown. The results from this approach fit well with the results when the full physical model of the wells is used in the simulation. The best fit would be obtained for a value of r_s of approximately 0.05.

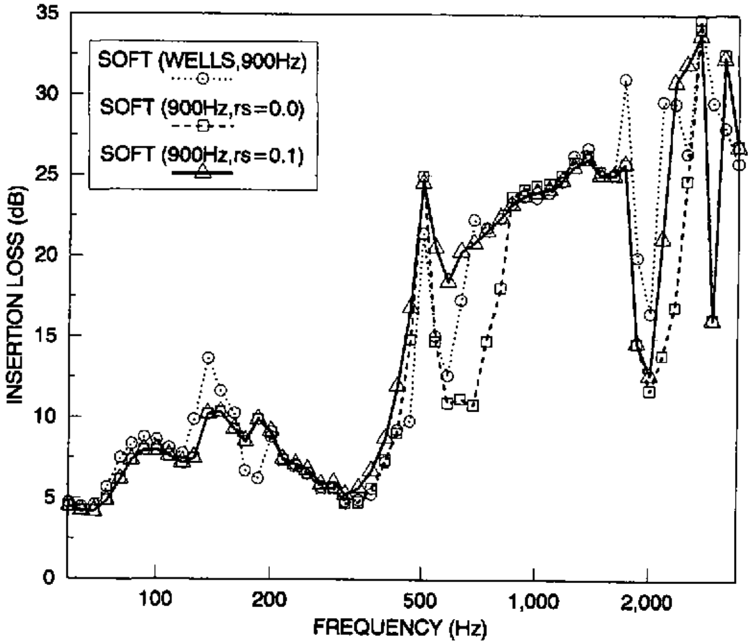

Fig. 3. Comparison of the results of the BE model for the barrier shown in Fig.2 with results for an equivalent barrier with a plane upper surface with admittance defined in Eq. (1).

In an attempt to improve the performance at low frequencies two types of well were incorporated in the upper surface of the cap, as shown in Fig. 4. In this case five wells of depth 0.20 m (tuned to a frequency of approximately 420 Hz) were used on the half of the cap closest to the source, and on the other half of the cap were seven wells of a depth of 0.10 m (tuned to a frequency of approximately 840 Hz).

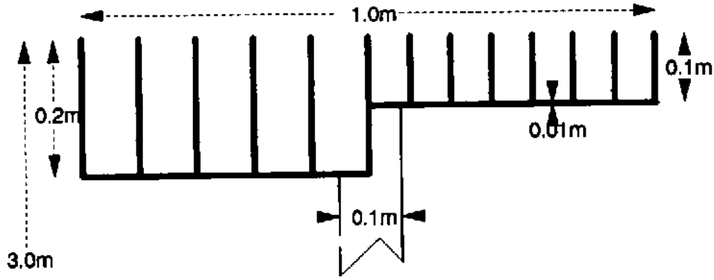

Fig. 4. Upper surface of a T-shaped barrier containing wells which are tuned to give pressure cancellation at the mouth at a frequencies of 420 and 840 Hz.

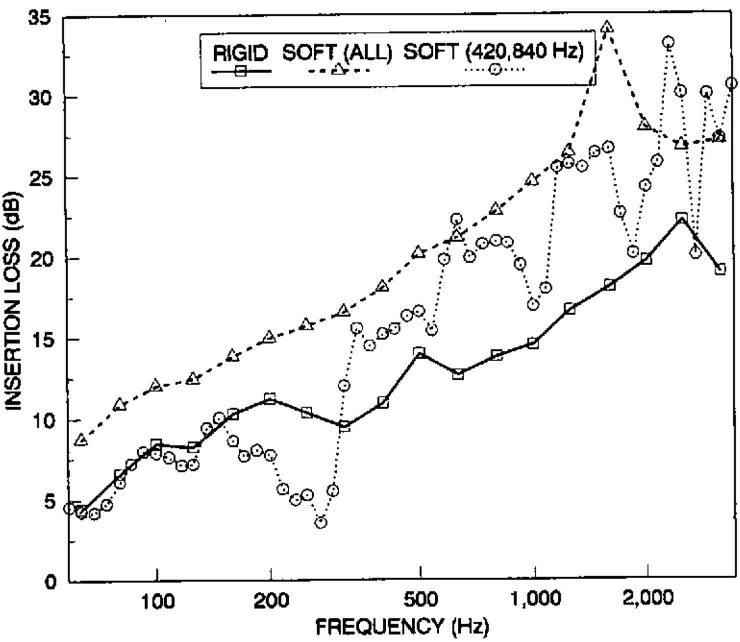

Fig. 5. Insertion loss spectra of a T-shaped barrier with an upper surface which is a)rigid, b)soft for all frequencies, and c)as shown in Fig. 4.

In Fig. 5 the resulting spectrum is shown. The region of high insertion loss has been extended to lower frequencies, from 600 to 300 Hz and this has removed part of the surface wave dip. However the reduction in the number of wells tuned to a particular frequency has reduced the efficiency of action as a soft surface, which occurs over the range from 300 to 1500 Hz.

This design was also modelled with a plane upper surface of the barrier with two regions of surface admittance defined as in Eq.(1) with an appropriate value of ℓ for each section. Again the agreement of this model with the results of the full physical model of the wells was excellent.

4. CONCLUSION

High values of insertion loss can be obtained from a T-shaped noise barrier when the upper surface is of the pressure release type. This can be achieved by introducing wells in the surface tuned to specific frequencies. It is found that for the well shapes investigated soft surface results were obtained over a significant range of frequencies. A surface wave effect was observed at lower frequencies. The performance of the wells can be described accurately in the boundary element model by the selection of an appropriate analytical expression for the admittance of the upper surface of the barrier, which is then assumed to be flat. The use of wells tuned to different frequencies can widen the spectral range over which the soft surface is effective.

References

[1] K.Fujiwara and N.Furuta, Sound Shielding Efficiency of a Barrier with a Cylinder at the Edge, *Noise Control Engineering Journal*, Vol. 37, No. 1, pp 5-11 (1991)

[2] D.H.Crombie, D.C.Hothersall and S.N.Chandler-Wilde, Multiple-Edge Noise Barriers, *Applied Acoustics*, Vol. 44, pp 353-367 (1995)

[3] D.C.Hothersall, S.N.Chandler-Wilde and M.N.Hajmirzae, Efficiency of Single Noise Barriers, *J.Sound Vib.*, Vol. 115, No. 4, pp 303-322 (1991)

[4] K.Fujiwara and E.Yotsumoto, Sound Shielding Efficiency of a Barrier with Soft Surface, *Proc. Internoise '90*, pp 343-346 (1990)